

Dear Christoph, Jake, and Jean,

Thank you for your thoughtful reviews and editorial comments. These, along with offline comments by Greg Johnson and other colleagues, have substantially improved our manuscript.

The reviewers appreciate the revisiting of this fundamental problem about the filling of the deep ocean, and the review of the PO<sub>4</sub>\* tracer, but raised concerns about some aspects of definition and suggested some useful caveats to our conclusions. As detailed in the comments below and in the revised manuscript with tracked changes, we have taken on almost all the review suggestions.

Jean Lynch-Steiglitz in RC2 provides a nice summary of the contribution of our manuscript and has no requests for edits, though supports the value of the comments of RC1 by Jake Gebbie.

Jake Gebbie in RC1 has several suggestions for edits, which we have addressed as discussed below.

*Definition of formation/contribution (RC1, Page C2)*

Jake encouraged us to be more explicit with definitions near the start of the manuscript and throughout. We have added a paragraph at the end of the introduction (lines 91-98) that explicitly states that we aim to derive estimates of the fraction of water in the deep Indo-Pacific from the North Atlantic vs the Southern Ocean, and that estimates of water or tracer flux require extra information and are discussed briefly at the end of the manuscript. We have also tightened up our description of water masses vs fluxes throughout the manuscript.

*16 Sv of NADW vs 45 Sv of Southern Water (RC1, Page C3 and first half C4)*

Jake made several very helpful points about the pitfalls of our discussion of Northern vs Southern water fluxes. Similar points were also made independently to us offline by Greg Johnson. To address these valid concerns we have removed this section of the manuscript (see line 100 in tracked changes). We also state Jake's points about not all of the ~16 Sv of NADW making it to the deep Indo-Pacific at lines 232-234, and the importance of residence time in consideration of water mass fraction vs flux at lines 241-244.

*The ventilated shelf water end-member in the Southern Ocean (RC1, second half page C4 and page C5)*

We have included at lines 176-185 the caveats made by Jake about the specificity of Weddell Shelf Water and the results of the exercise carried out by Johnson (2008). The idea of the water mass decomposition exercise is excellent, but we felt that going in to this in detail is beyond the scope and aim of this study; rather than being specific about the correct end-member decomposition, we wished to point out some of the issues of definition in this problem and how the previous estimates may be somewhat reconciled. However we have explicitly included the comment about the low salinity of the deep Indo-Pacific supporting a majority Southern Ocean source. We also highlight (lines 259-260) that while there are some clouds of points in areas of Figure 8, there are also striking linear features suggesting large portion of the deep ocean are well-described by predominantly two-component mixing.

*Grid box comment (RC1, end of page C5)*

We have edited this comment (now line 161) to be more in line with the description of Gebbie and Huybers (2010), that the use of gridded data may miss some small-scale features (such as overflow pathways), and so may miss some of the ventilated Southern Ocean end-member characteristics.

Alongside the changes in response to review comments described above, it was suggested by other colleagues that we elaborate on some of the features in the cross plots in the section on large scale features of the overturning circulation, and the link between  $\text{PO}_4^*$  (or preformed phosphate) and biological pump efficiency to add further interest to the conclusions. We have also made minor wording changes in some places for the sake of clarity. Finally, we have changed “North Atlantic” to “Southern Ocean” in the title (“What Fraction of the Pacific and Indian Oceans’ Deep Water is formed in the Southern Ocean?”), as we realized that the paper spends much more time discussing the Southern Ocean.

We thank the reviewers and editor for their time and consideration.

James Rae and Wally Broecker

1 | December 31, 2017, Revised 7 May 2018

2  
3  
4  
5

6 | **What Fraction of the Pacific and Indian Oceans' Deep Water**  
7 | **is formed in the Southern Ocean?**

8

9

10

11

12

13

14

15

16

17

18

19

20

21

22

23

24

25

26

27

28

29

30

31

32

33

34

James W.B. Rae  
School of Earth & Environmental Sciences  
Irvine Building  
University of St. Andrews  
St. Andrews  
KY16 9AL  
UK  
[jwbr@st-andrews.ac.uk](mailto:jwbr@st-andrews.ac.uk)

Wally Broecker  
Lamont-Doherty Earth Observatory of Columbia University  
61 Route 9W/PO Box 1000  
Palisades, NY 10964  
[broecker@ldeo.columbia.edu](mailto:broecker@ldeo.columbia.edu); (845) 365-8413 tel; (845) 365-8169 fax

Contribution to the  
Ernst Maier-Reimer Volume

James Rae 26/4/2018 14:25

**Deleted:** North Atlantic

36 **Abstract**

37 In this contribution we explore constraints on the fractions of deep water present in  
38 Indian and Pacific Oceans which originated in the northern Atlantic and in the Southern Ocean.  
39 Based on  $\text{PO}_4^*$  we show that if ventilated Antarctic shelf waters characterize the Southern  
40 contribution, then the proportions could be close to 50-50. If instead a Southern Ocean bottom  
41 water value is used, the Southern contribution is increased to 75 %. While this larger estimate  
42 may best characterize the volume of water entering the Indo-Pacific from the Southern Ocean, it  
43 contains a significant portion of entrained northern water. We also note that ventilation may be  
44 highly tracer dependent: for instance Southern Ocean waters may contribute only 35% of the  
45 deep radiocarbon budget, even if their volumetric contribution is 75%. In our estimation, the  
46 most promising approaches involve using CFC-11 to constrain the amount of deep water formed  
47 in the Southern Ocean. Finally, we highlight the broad utility of  $\text{PO}_4^*$  as a tracer of deep water  
48 masses, including descending plumes of Antarctic Bottom Water and large-scale patterns of deep  
49 ocean mixing, and as a tracer of the efficiency of the biological pump.

James Rae 7/5/2018 10:31

**Deleted:** are



51

52 **Remembering Ernst (W.B.)**

53 In 1987, Klaus Hasselmann was invited to Lamont-Doherty to present three lectures on  
54 climate. The first two dealt with what he referred to as PIPS and POPS. They didn't ring my bell.  
55 But the third one hit home. In it Klaus laid out the distribution of properties generated by Ernst  
56 Maier-Reimer's ocean circulation model (Maier-Reimer & Hasselmann, 1987). I was particularly  
57 interested in its ability to reproduce the distribution of natural radiocarbon in the ocean. But the  
58 plots he showed were at first look incomprehensible. It turned out, that rather than presenting  
59 differences from the <sup>14</sup>C to C ratio in atmospheric CO<sub>2</sub>, they were referenced to that in mean  
60 ocean water. After the lecture, I offered to come to Hamburg to help Maier-Reimer switch to a  
61 mode of presentation understandable to those conversant with the <sup>14</sup>C measurements. And so it  
62 was I spent three weeks with Ernst probing not only the <sup>14</sup>C to C distribution produced by his  
63 model, but also that of O<sub>2</sub> and SiO<sub>2</sub>. For me it was a fantastic learning experience. Not only did  
64 Ernst have an amazing mind but he had a knack of teaching by tweaking his model. Thus began  
65 a lasting collaboration and friendship.

66

67 **PO<sub>4</sub><sup>\*</sup>**

68 This led to an interest in determining the contributions of NADW and AABW to the  
69 ventilation of the deep Pacific and Indian Oceans. As the ratio of O<sub>2</sub> utilization to PO<sub>4</sub> release  
70 during respiration appears to be nearly constant throughout the ocean's interior (Takahashi et al.  
71 1985; Anderson & Sarmiento, 1994), Broecker and colleagues (Broecker et al., 1985, Broecker  
72 et al., 1998) proposed a conservative property PO<sub>4</sub><sup>\*</sup>:

73 
$$PO_4^* = PO_4 + \frac{O_2}{175} - 1.95 \mu\text{mol/kg}.$$

74 As only differences between PO<sub>4</sub><sup>\*</sup> values are of importance, the choice of the constant 1.95 is  
75 arbitrary. Hence zero would have been more convenient. Other choices for the O<sub>2</sub> consumption  
76 to PO<sub>4</sub> remineralisation ratio are also possible (Hupe & Karstensen, 2000), but have little impact

77 on our global-scale calculations, so we stick with the formulation of Broecker et al. (1998)  
78 above.

79 The attraction of  $\text{PO}_4^*$  as a water mass tracer is that although the deep waters formed in  
80 the northern Atlantic range widely in temperature, all the contributors have  $\text{PO}_4^*$  values close to  
81 0.7 (Figure 1). Further, the deep waters (i.e., >2000 m) in the deep Pacific and Indian Oceans  
82 have  $\text{PO}_4^*$  values close to 1.4. Hence were the  $\text{PO}_4^*$  for deep waters formed in the Southern  
83 Ocean known, the relative amounts of deep water produced in the two key source regions could  
84 be established.

85 Based on  $\text{PO}_4^*$ , Broecker et al. (1998) concluded that the deep Pacific and Indian Oceans  
86 received about half of their water from the northern Atlantic and half from the Southern Ocean.  
87 However, Johnson (2008), Gebbie & Huybers (2010), [Primeau & DeVries \(2011\)](#), and Khatiwala  
88 et al. (2012), using more complex inversions of multiple tracers and model-data synthesis,  
89 concluded that only about one quarter of this water came from the northern Atlantic.

90 Here we attempt to resolve this discrepancy by re-examining the  $\text{PO}_4^*$ -based approach.  
91 We show that much of the mismatch may be resolved by consideration of what “counts” as  
92 Southern-sourced water. Crucial to this discussion is the extent to which deep waters acquire  
93 their tracer signatures by ventilation in the surface ocean or by entrainment during descent. Our  
94 discussion is focussed on the volumetric contribution of Northern and Southern water masses to  
95 the deep Indo-Pacific, rather than water fluxes. Flux information – for tracers or for parcels of  
96 water – must be informed by estimates of residence time or formation rates, and we briefly  
97 discuss the potential of radiocarbon and CFCs to provide such information.

#### 99 $\text{PO}_4^*$ calculations revisited

100 Based on the GLODAPv2 dataset (Key et al., 2015; Olsen et al., 2016) we have re-  
101 examined deep ocean  $\text{PO}_4^*$  distributions. The mean  $\text{PO}_4^*$  value for deep (>2000 m) Indo-Pacific  
102 waters (Figure 2) is  $1.42 \pm 0.04$  (1 SD). We select waters below 2000 m as all determinations  
103 (Johnson, 2008; Gebbie and Huybers, 2010; Khatiwala et al., 2012) suggest that these depths are

James Rae 26/4/2018 15:17

**Deleted:** If the ~16 Sverdrups of NADW (Broecker et al. 1998; Ganachaud & Wunsch, 2000; Smethie and Fine, 2001) account for only one quarter of the water ventilating the Indian and Pacific Ocean, then the Southern Ocean must supply about 48 Sverdrups. On the other hand, if half the deep water ventilating the deep sea were produced in the northern Atlantic, then the required Southern Ocean ventilation flux would be reduced to about 16 Sverdrups. Quite a difference! -- [!]

116 predominantly a two-component mixture of deep North Atlantic and Southern Ocean waters. To  
117 help identify recently ventilated dense waters we also examined CFC11 and neutral density. The  
118 mean  $\text{PO}_4^*$  value for deep (>1500 m) recently ventilated (CFC11>0.5 pmol/kg) waters in the  
119 North Atlantic (Figure 2) is  $0.74 \pm 0.05$ . These Indo-Pacific and Atlantic end-members are  
120 within error of Broecker et al. (1998)'s values (1.39 and 0.73 respectively) and are relatively  
121 insensitive to choice of geographical boundaries, depth, CFC, and density limits.

122 Determining the  $\text{PO}_4^*$  end member of Southern Ocean deep waters is less  
123 straightforward. Broecker et al. (1998) use a  $\text{PO}_4^*$  value of 1.95. This value was obtained both  
124 by extrapolating the  $\text{PO}_4^* - \Theta$  relationship to the freezing point of sea water (Figure 1) and from  
125 direct observations of sinking surface waters in the Weddell and Ross Seas (Figure 3). The 1.95  
126  $\text{PO}_4^*$  value is achieved if water upwelling in the Southern Ocean is cooled to the freezing point,  
127 has about 65 percent of its  $\text{O}_2$  deficiency replenished, and loses little of its  $\text{PO}_4$  to sinking  
128 organics (see Table 1).

129 However while  $\text{PO}_4^*$  values of 1.95 characterize well-ventilated Antarctic shelf waters,  
130 these entrain up to three times their volume in circumpolar deep water as they cascade down the  
131 continental slope (Carmack & Foster, 1975; Orsi et al., 1999); indeed  $\text{PO}_4^*$  beautifully highlights  
132 this process (Figure 3). As a result, by the time Antarctic bottom water enters the ACC it has  
133 much lower  $\text{PO}_4^*$ : Weddell Sea bottom waters have  $\text{PO}_4^*$  of  $\sim 1.8$ , and deep Ross Sea waters  
134  $\sim 1.6$  (Figures 3 & 4). This basinal difference may be attributed to less input of NADW-  
135 influenced circumpolar deep water and higher local ventilation rates in the Weddell Sea,  
136 elevating  $\text{PO}_4^*$  in this more enclosed basin. The average circumpolar  $\text{PO}_4^*$  for recently  
137 ventilated (CFC-11 >0.5 pmol/kg) waters that have made it off the Antarctic shelf (>1500 m) and  
138 have neutral density higher than any North Atlantic waters (>28.3  $\text{kg/m}^3$ ) is  $1.64 \pm 0.07$  (1 SD;  
139 Figures 4 & 5).

140 Repeating Broecker et al.'s  $\text{PO}_4^*$  mass balance calculation with the Southern Ocean  
141 bottom water value of 1.65 suggests that the deep Indo-Pacific is filled by 75 % Southern-  
142 sourced water and 25 % NADW, with an uncertainty of  $\pm 9\%$  (1 SD). This is within error of the

143 values obtained by Johnson (2008), Gebbie and Huybers (2010) and Khatiwala et al. (2012).  
144 However if we use the well-ventilated shelf water value of 1.95, the north-south balance is closer  
145 to 50-50 (Broecker et al. 1998). This highlights that while the volume of what are typically  
146 considered southern deep waters in the Indo-Pacific may substantially outweigh that of NADW,  
147 much of this water is entrained in the subsurface and does not reflect full Southern Ocean  
148 ventilation. Note that while sinking waters in the North Atlantic also entrain surrounding waters  
149 on descent, these are of recent northern origin. Entrainment in the North Atlantic thus does not  
150 substantially influence the PO<sub>4</sub>\* signature of NADW nor the inference that this water is fully  
151 ventilated in the North Atlantic.

James Rae 30/4/2018 20:56

**Deleted:** :

James Rae 29/4/2018 22:28

**Deleted:** flux

James Rae 29/4/2018 22:28

**Deleted:** to

152 Differences in the extent to which the Southern Ocean end member is locally ventilated  
153 may thus explain much of the difference between the north-south balance obtained by Broecker  
154 et al. (1998) versus Johnson (2008), Gebbie & Huybers (2010), and Khatiwala et al. (2010).  
155 Johnson (2008) uses bottom water end member values for AABW, so it is unsurprising that our  
156 estimates using a Southern Ocean bottom water value are similar to his. Gebbie & Huybers  
157 (2008) and Khatiwala et al. (2010) use surface mixed layer conditions south of the ACC (Orsi et  
158 al., 1995), taken from gridded climatologies (WOA, Conkright et al., 1994; WOCE, Gouretski &  
159 Koltermann, 2004). As discussed by Gebbie & Huybers (2010), gridded data struggles to  
160 capture shelf features and dense overflow waters, and may thus miss some of the end member  
161 values characteristic of the ventilated Southern Ocean interior (Warren 1981). More crucially,  
162 high adiabatic upwelling rates (Toggweiler & Samuels, 1995; Marshall & Speer, 2012) and deep  
163 mixed layers (Gordon & Huber 1990; Dong et al., 2008) may also lead to inclusion of upwelled  
164 northern waters in these Southern end members, despite little property modification in the  
165 Southern Ocean surface. These issues may explain why the southern proportions of Gebbie &  
166 Huybers (2008) and Khatiwala et al. (2010) are larger than those using the ventilated PO<sub>4</sub>\*  
167 member (as in Broecker et al., 1998) and lie close to our estimates using bottom water PO<sub>4</sub>\*  
168 values.

James Rae 30/4/2018 00:20

**Deleted:** excludes

James Rae 7/5/2018 19:20

**Deleted:** most

James Rae 30/4/2018 00:20

**Deleted:** H

175 Note that we do not wish to imply that Antarctic shelf water is necessarily the most  
176 appropriate or only component to characterise ventilated Southern Ocean waters. As pointed out  
177 by Johnson (2008), shelf waters may have too unique a set of tracer properties to usefully capture  
178 the range of Southern Ocean water mass characteristics mixed into the deep Indo-Pacific.  
179 Furthermore while a 50-50 mixture between NADW and Antarctic shelf waters can produce the  
180 PO<sub>4</sub>\* signature of deep Indo-Pacific waters, it gives too high a salinity, so more Southern-sourced  
181 water is required. Processes besides shelf water formation may also help ventilate deep  
182 Southern-sourced waters, such as deep winter mixing in the open Southern Ocean (Gordon &  
183 Huber, 1990; Dong, 2008) and exchange along steeply dipping isopycnals in the Antarctic  
184 Circumpolar Current (Abernathy & Ferreira, 2015).

185 The key issue that we aim to bring awareness to is discussion of what “counts” as  
186 ventilated Southern water. Implicit in the Gebbie & Huybers (2008) and Khatiwala et al. (2010)  
187 studies is that any waters reaching the Southern Ocean mixed layer may be considered Southern  
188 Ocean waters. However these waters may experience little equilibration with Antarctic surface  
189 conditions, including cooling, gas exchange, and nutrient use, depending on their transit time  
190 through the Southern Ocean surface and the relaxation time of the tracer of interest. Therefore  
191 while they may count in the inventory of water volume entering the deep Indo-Pacific from the  
192 Southern Ocean (Talley 2013; Marshall & Speer 2012; Lumpkin & Speer 2007), they may only  
193 partially reflect the exchanges of heat and CO<sub>2</sub> key to the Southern Ocean’s role in climate  
194 (Stocker & Johnsen 2003; Marinov et al., 2006; Barker et al., 2009; Sigman et al., 2010; Ferrari  
195 et al. 2014).

### 197 **Ventilation and the Radiocarbon Budget**

198 The difference between Southern Ocean water mass volume and tracer ventilation is  
199 particularly pronounced in the deep radiocarbon budget. Of the 220 moles per year of <sup>14</sup>C  
200 undergoing radiodecay in the deep sea, about 20 moles/yr are resupplied by particle rain. As  
201 NADW supplies about 130 moles <sup>14</sup>C/yr, this leaves about 70 to be supplied from the Southern

James Rae 30/4/2018 21:09

**Deleted:** -

... [2]

James Rae 29/4/2018 22:43

**Deleted:** volume

James Rae 29/4/2018 22:42

**Deleted:** fluxes

James Rae 30/4/2018 20:53

**Deleted:** Timescales

James Rae 29/4/2018 22:58

**Deleted:** 16 Sverdrups of

James Rae 29/4/2018 22:58

**Deleted:** y

209 Ocean (see Table 2). Ventilation of radiocarbon is thus dominated by the North Atlantic, even if  
210 the Southern Ocean contributes greater volume. This is due to  $^{14}\text{C}$ 's long equilibration time and  
211 the limited exchange time between Southern Ocean surface waters and the atmosphere. Waters  
212 upwelled into the Southern Ocean surface thus do not reach equilibrium for  $^{14}\text{C}$  and radiocarbon  
213 gradients between surface and deep waters are very small (Broecker et al. 1985). This, along  
214 with the presence of  $^{14}\text{C}$  produced by H-bomb testing, also introduces large uncertainty into any  
215 attempt to use radiocarbon to quantify the contribution of Southern Ocean waters to the deep  
216 Indo-Pacific. The importance of northern versus southern ventilation may thus depend on the  
217 tracer and process of interest.

218

### 219 **Constraints Based on CFCs**

220 Further insights into Southern Ocean ventilation may be obtained using CFC data, which  
221 also offer the potential to constrain flux information. As with  $^{14}\text{C}$ , the degree of surface water  
222 saturation (Schlosser et al., 1991) must be carefully considered if the input flux of CFC tracer is  
223 to be converted to a ventilation flux for southern ocean water volume (England et al., 1994).  
224 However CFCs have the advantages over  $^{14}\text{C}$  of a much larger surface to deep gradient and faster  
225 and less complicated equilibration. CFC-based estimates of the flux of ventilated Southern  
226 Ocean water give values of  $\sim 15$  Sv (Orsi et al., 2002; Schlitzer 2007). This is similar to values  
227 for net production of NADW (Broecker et al., 1998; Ganachaud & Wunsch, 2000; Smethie &  
228 Fine, 2001), so appears to support roughly equal ventilation of the deep ocean by the northern  
229 Atlantic and the Southern Ocean (Broecker et al., 1998; Peacock et al., 2000; Orsi et al., 2001).  
230 However this does not rule out a much higher water flux from the south (Sloyan & Rintoul,  
231 2001; Lumpkin & Speer, 2007; Talley 2013) – just not full equilibrium with Southern Ocean  
232 surface conditions. Furthermore some of the  $\sim 16$  Sv of NADW may be lost to mixing or  
233 entrainment into Antarctic Intermediate or Bottom Waters (Primeau & Holzer, 2006), so the  
234 ventilation flux into the deep Indo-Pacific is likely still weighted towards the South. We also  
235 note that if diffusion down isopycnals in the open Southern Ocean is an important contributor to

James Rae 29/4/2018 23:00

**Deleted:** SO

James Rae 7/5/2018 18:29

**Deleted:** Indo-Pacific

James Rae 7/5/2018 18:30

**Deleted:** between

239 regional ventilation (Abernathy & Ferreira, 2015), this may not be as easily picked up as the  
240 CFC signal in shelf waters (Figure 5). The reason is that low CFC-11 concentrations in a large  
241 volume may match high CFC-11 concentrations in a small volume. Finally, even if the fluxes of  
242 Northern and Southern sourced waters into the deep Indo-Pacific are similar, it is possible for  
243 Southern-sourced waters to form a larger volumetric contribution if they have a longer residence  
244 time (Johnson 2008), which is quite plausible given their injection onto deeper density surfaces.

245

#### 246 **PO<sub>4</sub><sup>\*</sup> and other tracers of the global overturning circulation**

247 The large dynamic range of PO<sub>4</sub><sup>\*</sup> in the deep ocean makes it an effective tracer of the  
248 large scale circulation and mixing processes that make up the global overturning circulation. Its  
249 utility is highlighted by the PO<sub>4</sub><sup>\*</sup> sections, surfaces, and tracer-tracer plots in Figures 6-8,  
250 Supplementary Figures A1-6, and the SOCCOM data product (Verdy & Mazloff, 2017). As can  
251 be seen, low PO<sub>4</sub><sup>\*</sup> water from the North Atlantic mixes with high PO<sub>4</sub><sup>\*</sup> water formed in the  
252 Southern Ocean. This mixing occurs along shared isopycnals in the ACC (Figure 7; Abernathy  
253 & Ferreira, 2015), over rough seafloor topography (Naveira Garabato et al., 2004; Roemmich et  
254 al., 2009), and in the deep surface mixed layer of the Southern Ocean (Gordon & Huber 1990;  
255 Dong et al., 2008). These mixing patterns are also well illustrated on cross plots of PO<sub>4</sub><sup>\*</sup> with  
256 salinity and potential temperature (Figures 8 and A1-3). NADW is identifiable as a salinity and  
257 PO<sub>4</sub><sup>\*</sup> maximum sandwiched between fresher and higher PO<sub>4</sub><sup>\*</sup> southern waters above and below.  
258 Mixing between these Northern and Southern waters is well-illustrated by the linear trends in the  
259 PO<sub>4</sub><sup>\*</sup>-salinity plot (Figure 8). By the time circumpolar deep waters reach the Drake Passage,  
260 they have been somewhat homogenised, though a PO<sub>4</sub><sup>\*</sup> minimum at mid-depths remains, tracing  
261 the persistent influence of North Atlantic waters (Figure 6).

262 Other features of interest that are well highlighted by PO<sub>4</sub><sup>\*</sup> include: the input of very low  
263 PO<sub>4</sub><sup>\*</sup> deep water from the Mediterranean Sea into mid-depths of the North Atlantic (Figure 7 &  
264 A4); the penetration of relatively high PO<sub>4</sub><sup>\*</sup> water with a strong southern influence into the deep  
265 NE Atlantic (Figure 7, A1, A6); and the formation of mid-depth circumpolar deep waters

James Rae 30/4/2018 18:07

**Deleted:** and

James Rae 30/4/2018 22:31

**Deleted:** PO<sub>4</sub><sup>\*</sup> sections, surfaces, and tracer-tracer plots (Figures 7-9 and Supplementary Figures 1-6) also highlight patterns of circulation and mixing in the deep ocean

James Rae 30/4/2018 23:18

**Deleted:** 8

James Rae 30/4/2018 23:18

**Deleted:** 9

James Rae 30/4/2018 23:16

**Deleted:** 7

James Rae 30/4/2018 23:17

**Deleted:** 8

James Rae 30/4/2018 23:18

**Deleted:** 8

276 represented by a  $\text{PO}_4^*$  maxima, slightly underlying the salinity minimum of AAIW. Intermediate  
277 waters themselves are less readily identified by  $\text{PO}_4^*$ , forming in frontal regions with large  
278 nutrient gradients (Talley, 1993; Talley, 1996; Sarmiento et al., 2004), and are better traced by  
279 salinity (Figures 8, A1-3). Pacific deep waters returning through the Drake Passage are also hard  
280 to identify using  $\text{PO}_4^*$ , falling in the middle of a  $\text{PO}_4^*$  mixing gradient between northern and  
281 southern waters (Figure 7), and are better identified by their low oxygen and high silicate  
282 (Figures A3, A5, A6).

283 Alongside its use as a water mass tracer,  $\text{PO}_4^*$  may also provide complementary  
284 information on the carbon cycle. High  $\text{PO}_4^*$  waters, such as those found in the Southern Ocean,  
285 are subducted with high preformed phosphate and high oxygen; this indicates inefficient  
286 operation of the biological carbon pump and extensive ocean-atmosphere gas exchange, allowing  
287 net loss of  $\text{CO}_2$  from the ocean to the atmosphere.  $\text{PO}_4^*$  is close in formulation to preformed  
288 phosphate (Ito & Follows, 2005), but differs in not accounting for changes in oxygen uptake as a  
289 function of temperature and salinity, and making no assumption of initial oxygen saturation.  
290 Nonetheless, the ease with which  $\text{PO}_4^*$  can be calculated makes it a useful qualitative measure of  
291 the carbon cycle in the surface ocean, complementing its more quantitative use as a conservative  
292 water mass tracer at depth.

## 294 Conclusions

295 The use of  $\text{PO}_4^*$  to constrain the northern and southern contributions to the waters in the  
296 deep Indian and Pacific Oceans is highly dependent on the Southern Ocean end member value.  
297 Using end members characterizing ventilated Antarctic shelf waters versus Southern Ocean deep  
298 waters brackets the southern contribution to between 50 and 75 % respectively. There is value to  
299 both of these estimates: 75-25 may best characterize the ratio of deep Southern Ocean to North  
300 Atlantic water volume, while 50-50 may better represent the ratio of well-ventilated waters. In  
301 other words a large volume of the ocean's water experiences some degree of exposure to the

James Rae 30/4/2018 23:18  
**Deleted:** 9

James Rae 30/4/2018 23:18  
**Deleted:** s

James Rae 30/4/2018 23:18  
**Deleted:** 8

James Rae 1/5/2018 00:56  
**Formatted:** Subscript

James Rae 1/5/2018 00:56  
**Formatted:** Superscript

James Rae 1/5/2018 00:42  
**Deleted:** NADW

James Rae 1/5/2018 00:43  
**Deleted:** 2

James Rae 1/5/2018 00:43  
**Deleted:** :

James Rae 30/4/2018 00:06  
**Comment [1]:**

James Rae 1/5/2018 00:43  
**Deleted:** :

James Rae 1/5/2018 00:43  
**Deleted:** s

James Rae 1/5/2018 00:43  
**Deleted:** fluxes

James Rae 1/5/2018 00:44  
**Deleted:** , as supported by CFC input models



312 Southern Ocean surface, but the volume of those taking on a more completely ventilated  
313 Southern Ocean signal is much smaller.

314

315 **Acknowledgments**

316 We thank Jake Gebbie and Jean Lynch-Steiglitz for their thoughtful reviews, and Jake  
317 Gebbie, Greg Johnson, and Jess Adkins for helpful discussions, all of which substantially  
318 improved this manuscript. We also thank Matthew Mazloff for making  $\text{PO}_4^*$  available as part of  
319 the B-SOSE product ([http://sose.ucsd.edu/BSOSE\\_iter105\\_solution.html](http://sose.ucsd.edu/BSOSE_iter105_solution.html)). W.B. acknowledges  
320 funding from the Comer Science and Education Foundation. mJ.W.B.R. acknowledges funding  
321 from NERC standard grants NE/N003861/1 and NE/N011716/1, and support from the School of  
322 Earth and Environmental Sciences at the University of St Andrews during W.B.'s visit, which  
323 sparked the discussions that led to this paper.

324

325  
326  
327  
328  
329  
330  
331  
332  
333  
334  
335  
336  
337  
338  
339  
340  
341  
342  
343  
344

**Table 1. Expected PO<sub>4</sub><sup>\*</sup>**

Upwelled PO<sub>4</sub> = 2.2 μmol/kg  
Upwelled O<sub>2</sub> = 210 μmol/kg  
Saturation O<sub>2</sub> = 360 μmol/kg

Assume

- 1) No PO<sub>4</sub> utilization
- 2) 65% O<sub>2</sub> resaturation

Then

$$PO_4^* = 2.2 + \frac{0.65(360-210)+210}{175} - 1.95 = 1.95 \mu\text{mol/kg}$$

**Table 2.** Example  $^{14}\text{C}$  budget for ~25% NADW contribution.

---

<b>Loss via Radiodecay</b>	
Volume of deep sea	$8 \times 10^{17} \text{ m}^3$
Mean $\Sigma\text{CO}_2$	2.3 moles/ $\text{m}^3$
Mean $\Delta^{14}\text{C}$	-175‰
Mean $^{14}\text{C}/\text{C}$	$1.0 \times 10^{-12}$
Amount of $^{14}\text{C}$ in deep sea	$1.8 \times 10^6$ moles
Amount decaying	220 moles/yr
<b>Gain of Radiocarbon from North Atlantic</b>	
Flux	16 Sverdrups
Flux	$6 \times 10^{14} \text{ m}^3/\text{yr}$
$\Sigma\text{CO}_2$	2.1 moles/ $\text{m}^3$
$\Delta^{14}\text{C}$	-67‰
$^{14}\text{C}/\text{C}$ - $^{14}\text{C}/\text{C}$ mean deep sea	$0.13 \times 10^{-12}$
Input $^{14}\text{C}$ to deep sea	130 moles/yr
<b>Gain of Radiocarbon from Southern Ocean</b>	
Flux	45 Sverdrups
Flux	$17 \times 10^{14} \text{ m}^3/\text{yr}$
$\Sigma\text{CO}_2$	2.2 moles/yr
$\Delta^{14}\text{C}$	-154‰
$^{14}\text{C}/\text{C}$ - $^{14}\text{C}/\text{C}$ mean deep sea	$0.025 \times 10^{-12}$
Input $^{14}\text{C}$ to deep sea	70 moles/yr
<b>Gain of Radiocarbon by Particle Flux</b>	
Carbon flux	$0.5 \text{ moles}/\text{m}^2/\text{yr}$
$\Delta^{14}\text{C}$	-70‰
$^{14}\text{C}/\text{C}$ - $^{14}\text{C}/\text{C}$ mean deep sea	$0.126 \times 10^{-12}$
Input $^{14}\text{C}$ to deep sea	20 moles/yr
<b>Total Gain of Radiocarbon</b>	220 moles/yr

---

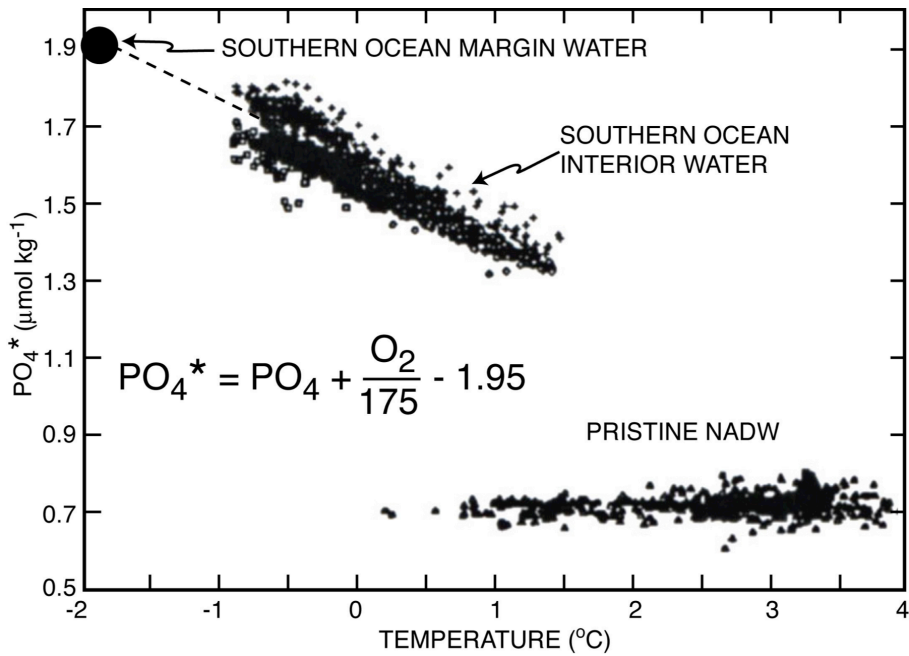


Figure 1. Plots of  $PO_4^*$  versus potential temperature for water formed in the northern Atlantic and in the Southern Ocean (based on measurements made as part of the GEOSECS expeditions). Note that all contributors of NADW have  $PO_4^*$  values within the measurement error of  $0.75 \mu\text{mol/kg}$ . The Southern Ocean  $PO_4^*$  was originally obtained by extrapolating the observed  $PO_4^*$  - temperature trend to sea water's freezing point (Table 1). As shown in Figures 3 and 4, this extrapolated value is consistent with values observed close to the Antarctic margin in the Weddell Sea.

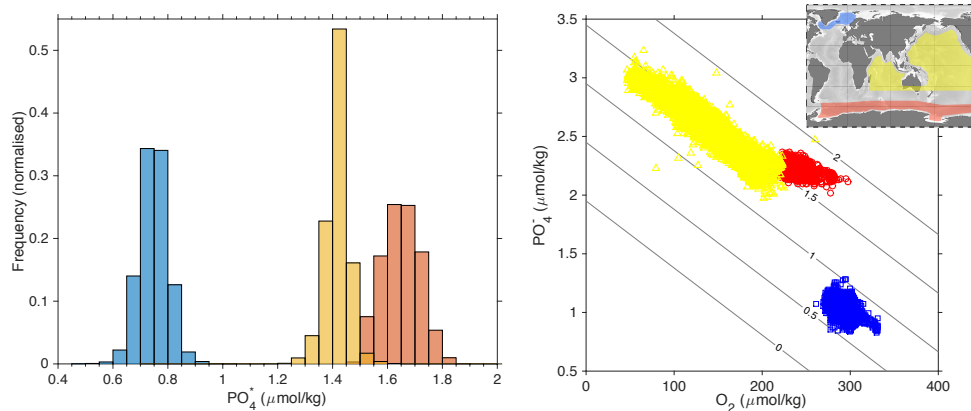


Figure 2: End member  $\text{PO}_4^*$  values for deep North Atlantic waters (blue) and deep Southern Ocean waters (red), along with deep Indo-Pacific waters (yellow). Data are from GLODAPv2 (Key et al., 2015; Olsen et al., 2016) and taken from the regions shown in the inset map. North Atlantic data are  $>1500$  m and have  $\text{CFC11} > 0.5$  pmol/kg; Southern Ocean data are  $>1500$  m, have  $\text{CFC11} > 0.5$  pmol/kg, and neutral density  $>28.3$  kg/m<sup>3</sup> (see Figure 4); Indo-Pacific data are  $>2000$  m. Normalised histograms of  $\text{PO}_4^*$  are shown for each region in the left hand panel, and the corresponding  $\text{O}_2$  and  $\text{PO}_4^*$  concentrations on the right, contoured with  $\text{PO}_4^*$ .

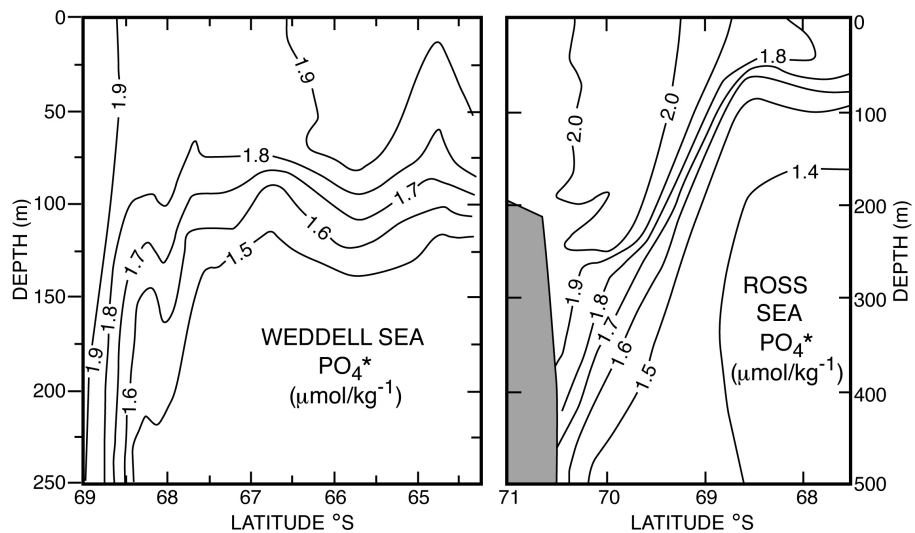


Figure 3.  $\text{PO}_4^*$  sections extending out from the Antarctic continent for the Weddell and Ross Seas. As can be seen, water with a value close to 1.95 is descending in a narrow margin-hugging plume.

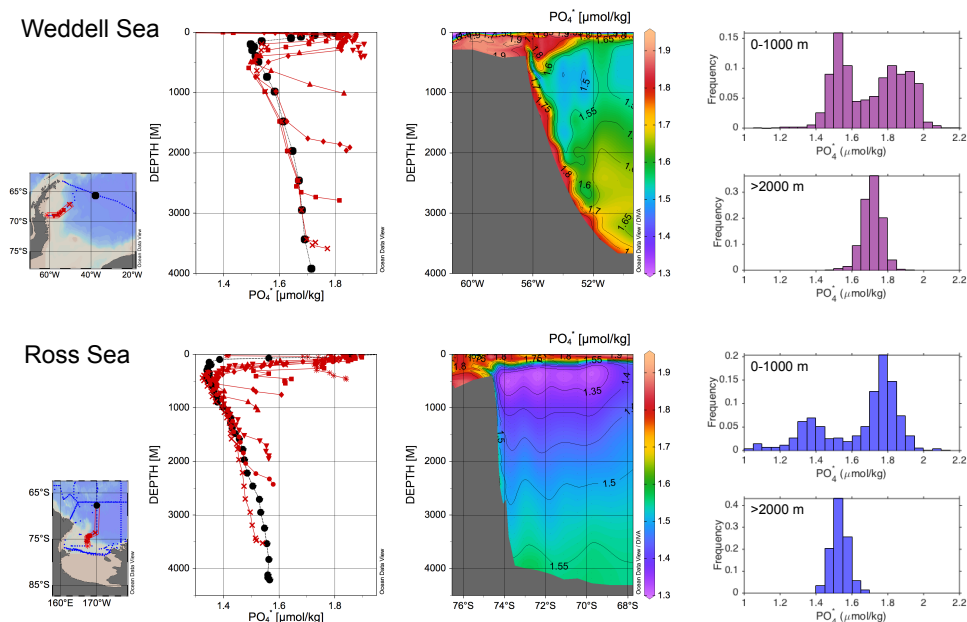


Figure 4:  $\text{PO}_4^*$  data in the Weddell and Ross Seas from the GLODAPv2 database. Sections (central panel) show high  $\text{PO}_4^*$  values on the shelves, that descend the continental margin in a narrow plume (Warren 1981). This is also picked out by selected depth profiles along these sections (left hand panel), with the black dots showing a profile further out from the shelf edge. Entrainment of low  $\text{PO}_4^*$  waters in the subsurface reduces southern deep water  $\text{PO}_4^*$ , from 1.95 on the shelf to  $\sim 1.65$  at depth. This can also be seen in the histograms in the right hand panel (encompassing larger areas than those shown in the maps and sections), which show two distinct  $\text{PO}_4^*$  populations in the top 1000 m, which mix to give the more homogenous values at depth. Note that Weddell Sea waters have higher  $\text{PO}_4^*$  than Ross Sea waters, likely due to less influence of low- $\text{PO}_4^*$  NADW and higher local deep water formation rates, elevating  $\text{PO}_4^*$  throughout this more enclosed basin. Data are from GLODAPv2 (Key et al., 2015; Olsen et al., 2016) with profiles, maps, and sections plotted in ODV (Schlitzer 2015), with sections contoured using isopycnic gridding.

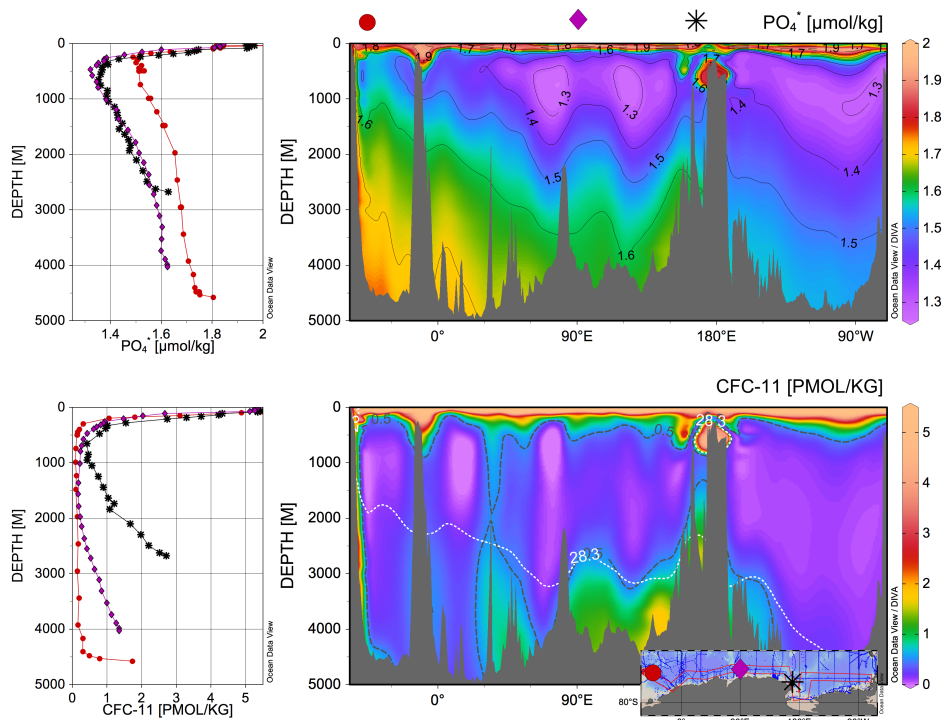


Figure 5. Circum Antarctic sections of  $\text{PO}_4^*$  and CFC-11 through the southern portion of the Southern Ocean. The locations of the profiles in the left hand panel are illustrated with symbols and shown in the inset map: the red circles are from the Weddell Sea, the purple diamonds from the Antarctic margin in the Indian sector, and the black stars from the northern margin of the Ross Sea. In the CFC section the black dashed line indicates CFC-11 concentrations  $>0.5$  pmol/kg and the white dotted line indicates neutral densities  $>28.3$  kg/m<sup>3</sup>; these criteria, along with depth  $>1500$  m, are used to define the alternative deep Southern Ocean  $\text{PO}_4^*$  end member. Data are from GLODAPv2 (Key et al., 2015; Olsen et al., 2016) with profiles, maps, and sections plotted in ODV (Schlitzer 2015), with sections contoured using isopycnic gridding.



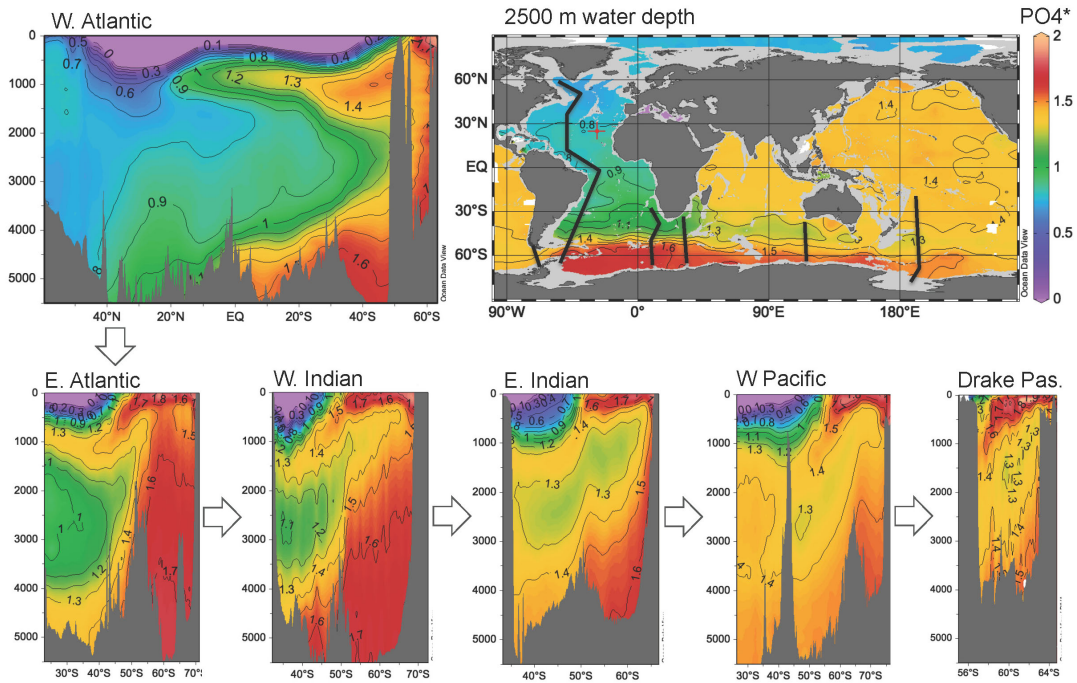


Figure 6.  $PO_4^*$  sections for the western Atlantic and for a series of quadrants of the Southern Ocean. Low  $PO_4^*$  waters entering the Southern Ocean from the Atlantic and the high  $PO_4^*$  waters generated in the Southern Ocean are blended in the Antarctic Circumpolar Current, forming circumpolar deep water. However a  $PO_4^*$  high at the seafloor and low at ~2000 m continue to trace the influence of AABW and NADW respectively. Data are from GLODAPv2 (Key et al., 2015; Olsen et al., 2016) with profiles, maps, and sections plotted in ODV (Schlitzer 2015), with sections contoured using isopycnic gridding.

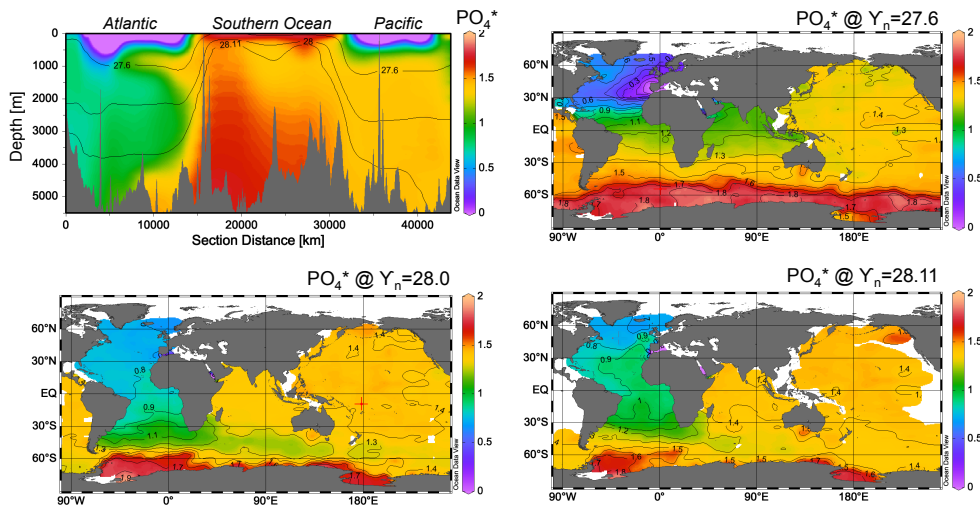


Figure 7.  $PO_4^*$  on a section through the Atlantic, Southern, and Pacific Oceans and on the 27.6, 28.0, and 28.11 isopycnal horizons. The depths of these horizons are shown in the section. Mixing of low  $PO_4^*$  from the North and high  $PO_4^*$  from the South takes place along shared isopycnals, and also diapycnally in the Southern Ocean mixed layer and over rough bottom topography. Data are from GLODAPv2 (Key et al., 2015; Olsen et al., 2016) with profiles, maps, and sections plotted in ODV (Schlitzer 2015).

James Rae 1/5/2018 00:44  
 Deleted: 8

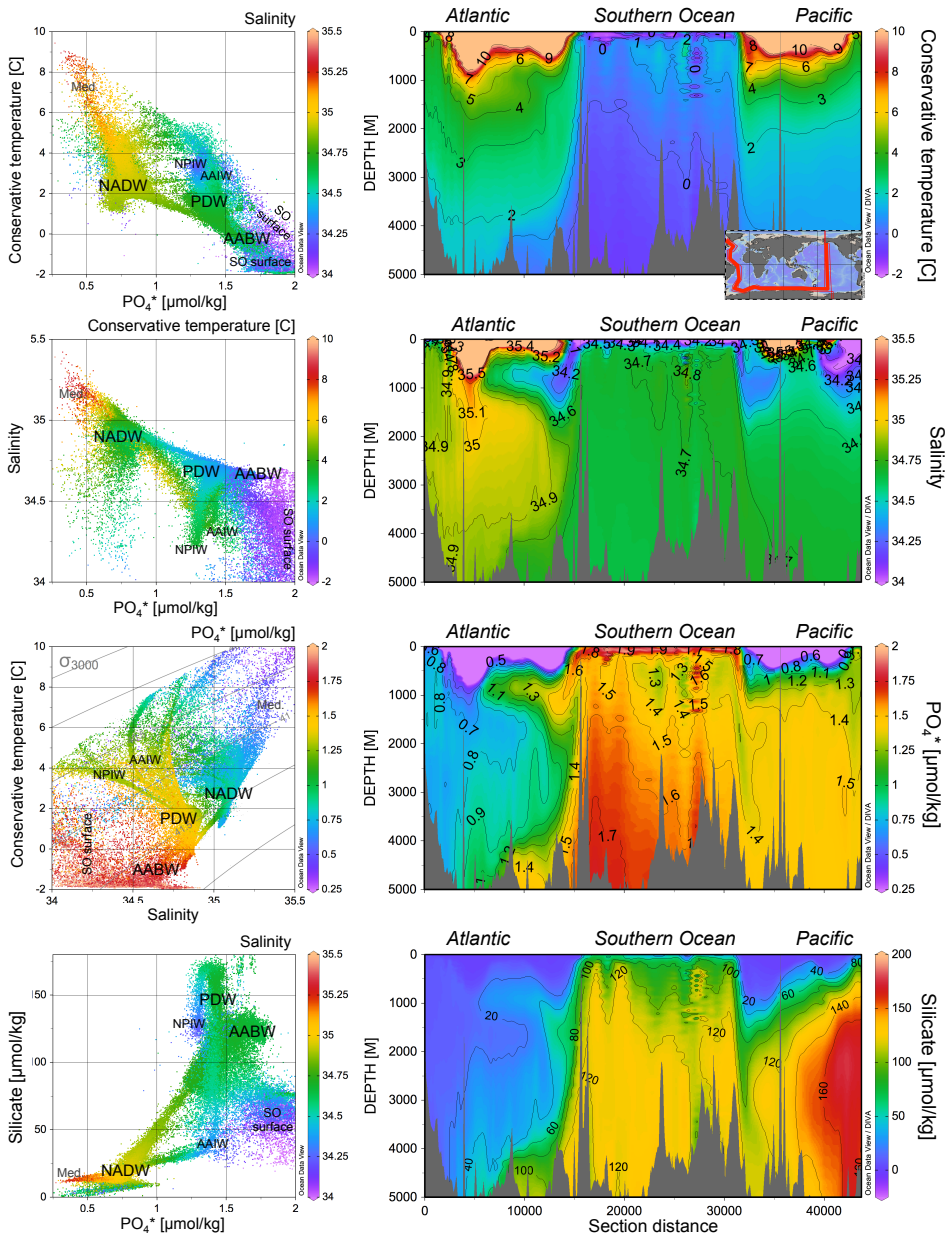


Figure 8: A global hydrographic section for potential temperature, salinity,  $PO_4^*$ , and silicate. Cross plots show all the data in this section with neutral density greater than  $27.2 \text{ kg/m}^3$ ; the colours of the dots refer to the scale shown to the right of the cross plots. Data are from GLODAPv2 (Key et al., 2015; Olsen et al., 2016) with profiles, maps, and sections plotted in ODV (Schlitzer 2015), with sections contoured using isopycnic gridding.

James Rae 1/5/2018 00:45

Deleted: 9

## References

- Abernathey, R. and Ferreira, D., 2015. Southern Ocean isopycnal mixing and ventilation changes driven by winds. *Geophysical Research Letters*, 42(23).
- Anderson, L.A. and Sarmiento, J.L., 1994. Redfield ratios of remineralization determined by nutrient data analysis. *Global biogeochemical cycles*, 8(1), pp.65-80.
- Barker, S., Diz, P., Vautravers, M.J., Pike, J., Knorr, G., Hall, I.R. and Broecker, W.S., 2009. Interhemispheric Atlantic seesaw response during the last deglaciation. *Nature*, 457(7233), pp.1097-1102.
- Broecker, W.S., Takahashi, T. and Takahashi, T., 1985. Sources and flow patterns of deep-ocean waters as deduced from potential temperature, salinity, and initial phosphate concentration. *Journal of Geophysical Research: Oceans*, 90(C4), pp.6925-6939.
- Broecker, W.S., Peng, T.H., Ostlund, G. and Stuiver, M., 1985. The distribution of bomb radiocarbon in the ocean. *Journal of Geophysical Research: Oceans*, 90(C4), pp.6953-6970.
- Broecker, W.S., Peacock, S., Walker, S., Weiss, R., Fahrback, E., Schroeder, M., Mikolajewicz, U., Heinze, C., Carmack, E.C. and Foster, T.D., 1975, November. On the flow of water out of the Weddell Sea. In *Deep Sea Research and Oceanographic Abstracts* (Vol. 22, No. 11, pp. 711-724). Elsevier.
- Conkright, M.E., Boyer, T.P. and Levitus, S., 1994. World Ocean Atlas: 1994 Nutrients (Vol. 1). DIANE Publishing.
- [DeVries, T. and Primeau, F., 2011. Dynamically and observationally constrained estimates of water-mass distributions and ages in the global ocean. \*Journal of Physical Oceanography\*, 41\(12\), pp.2381-2401.](#)
- Dong, S., Sprintall, J., Gille, S.T. and Talley, L., 2008. Southern Ocean mixed-layer depth from Argo float profiles. *Journal of Geophysical Research: Oceans*, 113(C6).
- England, M.H., 1995. Using chlorofluorocarbons to assess ocean climate models. *Geophysical Research Letters*, 22(22), pp.3051-3054.
- Ferrari, R., Jansen, M.F., Adkins, J.F., Burke, A., Stewart, A.L. and Thompson, A.F., 2014. Antarctic sea ice control on ocean circulation in present and glacial climates. *Proceedings of the National Academy of Sciences*, 111(24), pp.8753-8758.
- Key, R., Peng, T.-H., Rubin, S. 1998. How much deep water is formed in the Southern Ocean? *J. Geophys. Res.* 103, 15,833-15,843.
- Ganachaud, A. and Wunsch, C., 2000. Improved estimates of global ocean circulation, heat transport and mixing from hydrographic data. *Nature*, 408(6811), pp.453-457.
- Gebbie, G., Huybers, P. 2010. Total matrix intercomparison: A method for determining the geometry of water-mass pathways. *J. Phys. Oceanography* 40, 1710-1728.
- Gordon, A.L. and Huber, B.A., 1990. Southern Ocean winter mixed layer. *Journal of Geophysical Research: Oceans*, 95(C7), pp.11655-11672.

- Gouretski, V. and Koltermann, K.P., 2004. WOCE global hydrographic climatology. *Berichte des BSH*, 35, pp.1-52.
- Hupe, A. and Karstensen, J., 2000. Redfield stoichiometry in Arabian Sea subsurface waters. *Global Biogeochemical Cycles*, 14(1), pp.357-372.
- Johnson, G.C., 2008. Quantifying Antarctic bottom water and North Atlantic deep water volumes. *Journal of Geophysical Research: Oceans*, 113(C5).
- Key, R.M., Olsen, A., van Heuven, S., Lauvset, S.K., Velo, A., Lin, X., Schirnack, C., Kozyr, A., Tanhua, T., Hoppema, M. and Jutterström, S., 2015. Global Ocean Data Analysis Project, Version 2 (GLODAPv2).
- Khatiwala, S., Primeau, F., Holzer, M. 2012. Ventilation of the deep ocean constrained with tracer observations and implications for radiocarbon estimates of ideal mean age. *Earth Planet. Sci. Lett.* 325-326, 116-125.
- Lumpkin, R. and Speer, K., 2007. Global ocean meridional overturning. *Journal of Physical Oceanography*, 37(10), pp.2550-2562.
- Maier-Reimer, E. and Hasselmann, K., 1987. Transport and storage of CO<sub>2</sub> in the ocean—an inorganic ocean-circulation carbon cycle model. *Climate dynamics*, 2(2), pp.63-90.
- Marinov, I., Gnanadesikan, A., Toggweiler, J.R. and Sarmiento, J.L., 2006. The southern ocean biogeochemical divide. *Nature*, 441(7096), pp.964-967.
- Marshall, J. and Speer, K., 2012. Closure of the meridional overturning circulation through Southern Ocean upwelling. *Nature Geoscience*, 5(3), pp.171-180.
- Naveira-Garabato, A.C.N., Polzin, K.L., King, B.A., Heywood, K.J. and Visbeck, M., 2004. Widespread intense turbulent mixing in the Southern Ocean. *Science*, 303(5655), pp.210-213.
- Olsen, A., Key, R.M., van Heuven, S., Lauvset, S.K., Velo, A., Lin, X., Schirnack, C., Kozyr, A., Tanhua, T., Hoppema, M. and Jutterström, S., 2016. The Global Ocean Data Analysis Project version 2 (GLODAPv2)—an internally consistent data product for the world ocean. *Earth System Science Data*, 8(2), p.297.
- Orsi, A.H., Johnson, G.C. and Bullister, J.L., 1999. Circulation, mixing, and production of Antarctic Bottom Water. *Progress in Oceanography*, 43(1), pp.55-109.
- Orsi, A.H., Jacobs, S.S., Gordon, A.L. and Visbeck, M., 2001. Cooling and ventilating the abyssal ocean. *Geophysical Research Letters*, 28(15), pp.2923-2926.
- Orsi, A.H., Smethie, W.M. and Bullister, J.L., 2002. On the total input of Antarctic waters to the deep ocean: A preliminary estimate from chlorofluorocarbon measurements. *Journal of Geophysical Research: Oceans*, 107(C8).
- Peacock, S., Visbeck, M. and Broecker, W., 2000. Deep water formation rates inferred from global tracer distributions: An inverse approach. *Inverse Methods in Global Biogeochemical Cycles*, pp.185-195.
- [Primeau, F., and M. Holzer, 2006: The ocean's memory of the atmosphere: Residence- time and ventilation-rate distributions of water masses. \*J. Phys. Oceanogr.\*, 36, 1439– 1456.](#)

- Roemmich, D., Johnson, G.C., Riser, S., Davis, R., Gilson, J., Owens, W.B., Garzoli, S.L., Schmid, C. and Ignaszewski, M., 2009. The Argo Program: Observing the global ocean with profiling floats. *Oceanography*, 22(2), pp.34-43.
- Sarmiento, J.Á., Gruber, N., Brzezinski, M.A. and Dunne, J.P., 2004. High-latitude controls of thermocline nutrients and low latitude biological productivity. *Nature*, 427(6969), pp.56-60.
- Schlitzer, R., 2007. Assimilation of radiocarbon and chlorofluorocarbon data to constrain deep and bottom water transports in the world ocean. *Journal of Physical Oceanography*, 37(2), pp.259-276.
- Schlitzer, R., Ocean Data View, <http://odv.awi.de>, 2015.
- Schlosser, P., Bonisch, G., Rhein, M. and Bayer, R., 1991. Reduction of Deepwater Formation in the Greenland Sea during the 1980's. *Evidence from Tracer Data, Science*, 251, p.1054.
- Sigman, D.M., Hain, M.P. and Haug, G.H., 2010. The polar ocean and glacial cycles in atmospheric CO<sub>2</sub> concentration. *Nature*, 466(7302), pp.47-55.
- Sloyan, B.M. and Rintoul, S.R., 2001. The Southern Ocean limb of the global deep overturning circulation. *Journal of Physical Oceanography*, 31(1), pp.143-173.
- Smethie, W.M. and Fine, R.A., 2001. Rates of North Atlantic Deep Water formation calculated from chlorofluorocarbon inventories. *Deep Sea Research Part I: Oceanographic Research Papers*, 48(1), pp.189-215.
- Stocker, T.F. and Johnsen, S.J., 2003. A minimum thermodynamic model for the bipolar seesaw. *Paleoceanography*, 18(4).
- Takahashi, T., Broecker, W.S. and Langer, S., 1985. Redfield ratio based on chemical data from isopycnal surfaces. *Journal of Geophysical Research: Oceans*, 90(C4), pp.6907-6924.
- Talley, L.D., 1993. Distribution and formation of North Pacific intermediate water. *Journal of Physical Oceanography*, 23(3), pp.517-537.
- Talley, L.D., 1996. Antarctic intermediate water in the South Atlantic. *The South Atlantic: Present and Past Circulation*, pp.219-238.
- Talley, L.D., 2013. Closure of the global overturning circulation through the Indian, Pacific, and Southern Oceans: Schematics and transports. *Oceanography*, 26(1), pp.80-97.
- Toggweiler, J.R. and Samuels, B., 1995. Effect of Drake Passage on the global thermohaline circulation. *Deep Sea Research Part I: Oceanographic Research Papers*, 42(4), pp.477-500.
- [A. Verdy and M. Mazloff, 2017: A data assimilating model for estimating Southern Ocean biogeochemistry. \*J. Geophys. Res. Oceans.\*, 122, doi:10.1002/2016JC012650.](#)
- Warren, B.A., 1981. Deep circulation of the world ocean. *Evolution of physical oceanography*, pp.6-41.



# Appendix Figures

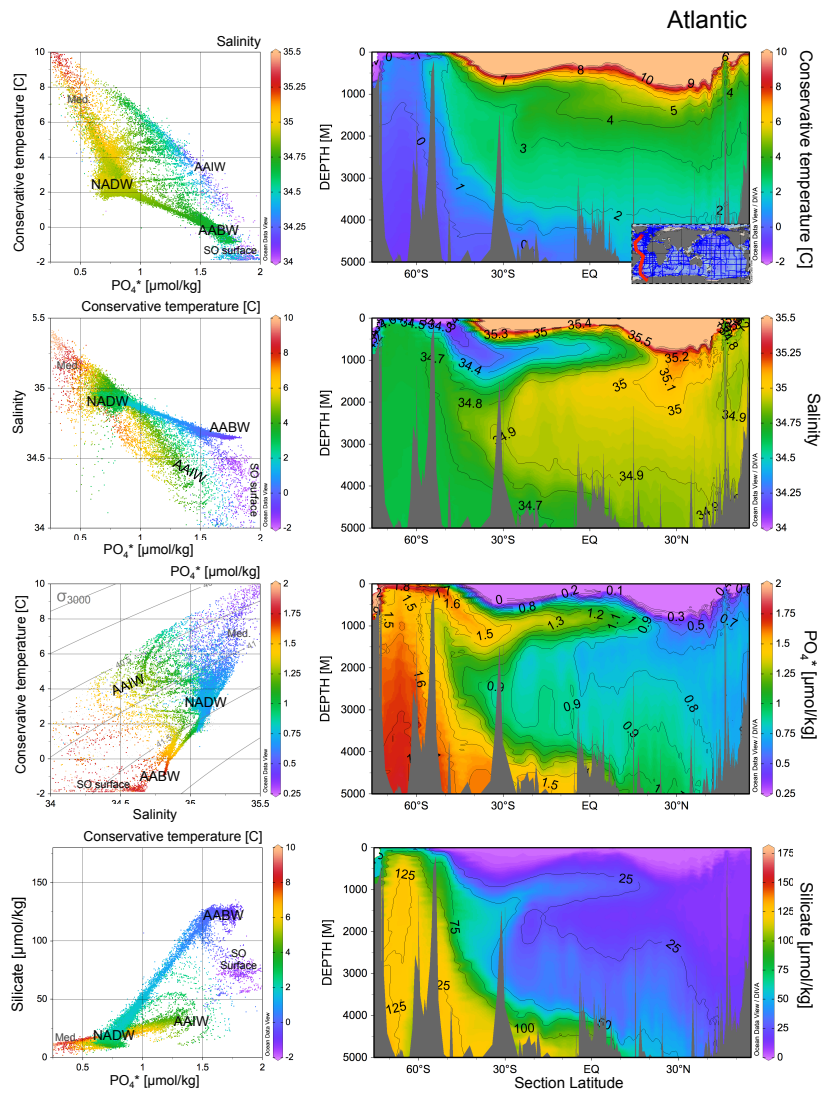


Figure A1: Atlantic hydrographic section for potential temperature, salinity,  $PO_4^*$ , and silicate. Cross plots show all the data in this section with neutral density greater than  $27.2 \text{ kg/m}^3$ ; the colours of the dots refer to the scale shown to the right of the cross plots. Data are from GLODAPv2 (Key et al., 2015; Olsen et al., 2016) with profiles, maps, and sections plotted in ODV (Schlitzer 2015), with sections contoured using isopycnic gridding.

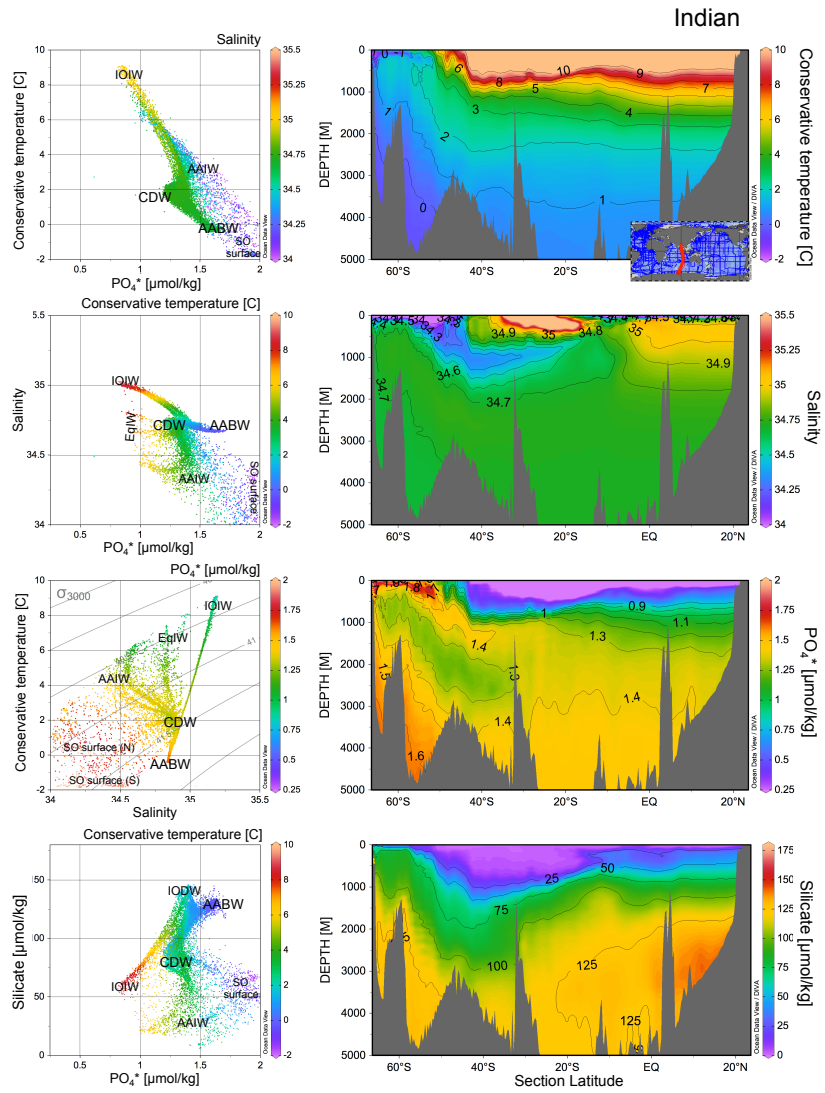


Figure A2: Indian Ocean hydrographic section for potential temperature, salinity,  $\text{PO}_4^*$ , and silicate. Cross plots show all the data in this section with neutral density greater than  $27.2 \text{ kg/m}^3$ ; the colours of the dots refer to the scale shown to the right of the cross plots. Data are from GLODAPv2 (Key et al., 2015; Olsen et al., 2016) with profiles, maps, and sections plotted in ODV (Schlitzer 2015), with sections contoured using isopycnal gridding.



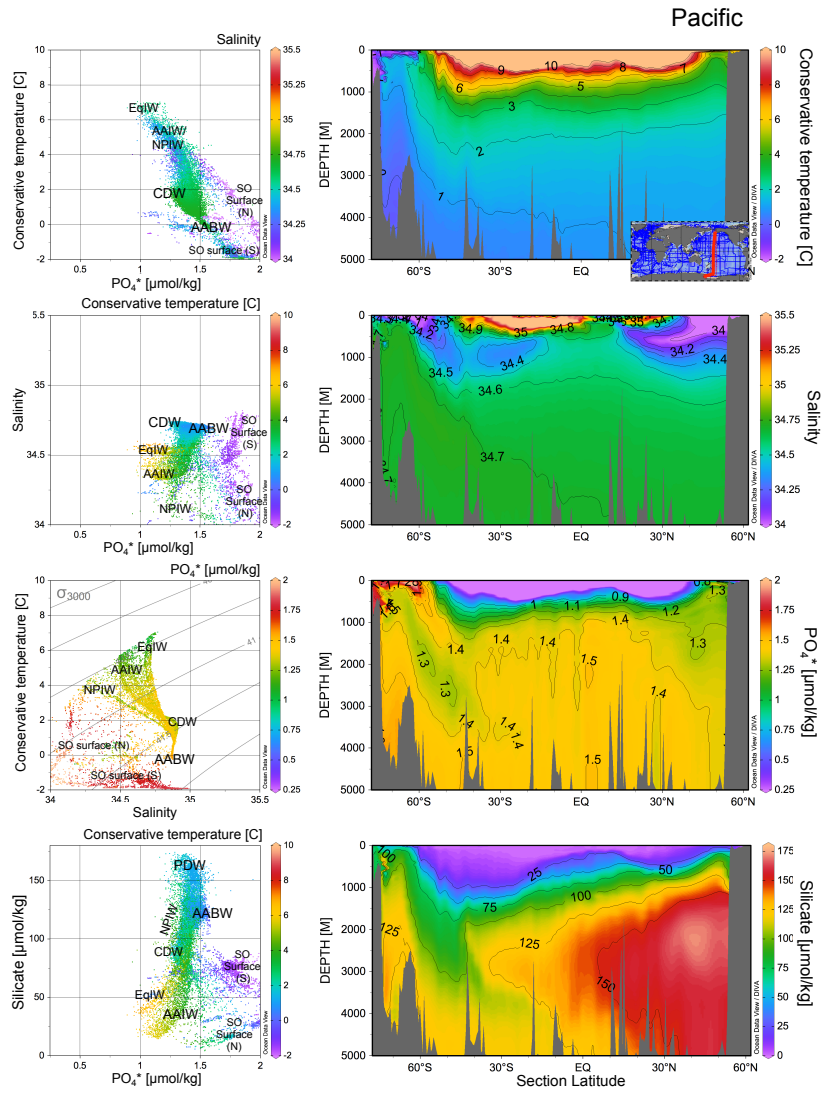


Figure A3: Pacific hydrographic section for potential temperature, salinity,  $PO_4^*$ , and silicate. Cross plots show all the data in this section with neutral density greater than  $27.2 \text{ kg/m}^3$ ; the colours of the dots refer to the scale shown to the right of the cross plots. Data are from GLODAPv2 (Key et al., 2015; Olsen et al., 2016) with profiles, maps, and sections plotted in ODV (Schlitzer 2015), with sections contoured using isopycnic gridding.

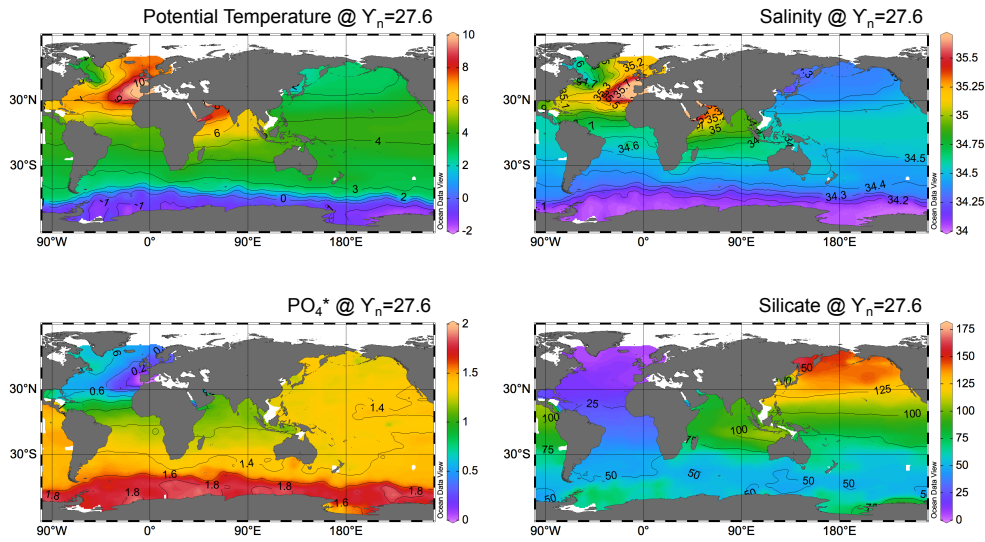


Figure A4: Potential temperature, salinity,  $PO_4^*$ , and silicate on the 27.6 isopycnal horizon. The depth of this horizon is shown in Figure 8 and averages  $\sim 1000$  m in the basins and is in the mixed layer in the Southern Ocean. Data are from GLODAPv2 (Key et al., 2015; Olsen et al., 2016) with profiles, maps, and sections plotted in ODV (Schlitzer 2015).

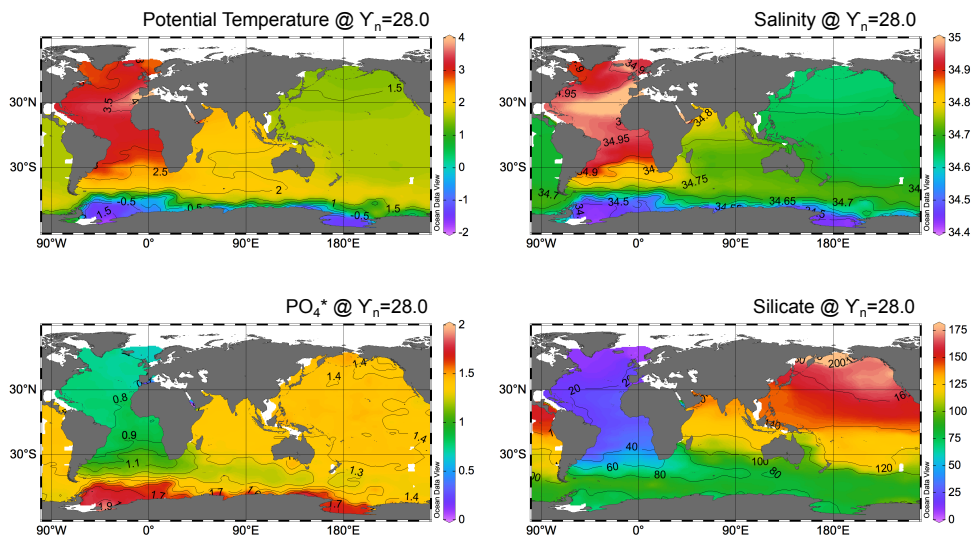


Figure A5: Potential temperature, salinity,  $PO_4^*$ , and silicate on the 28.0 isopycnal horizon. The depth of this horizon is shown in Figure 8 and averages  $\sim 2500$  m in the basins and  $\sim 250$  m in the mixed layer in the Southern Ocean. Data are from GLODAPv2 (Key et al., 2015; Olsen et al., 2016) with profiles, maps, and sections plotted in ODV (Schlitzer 2015).

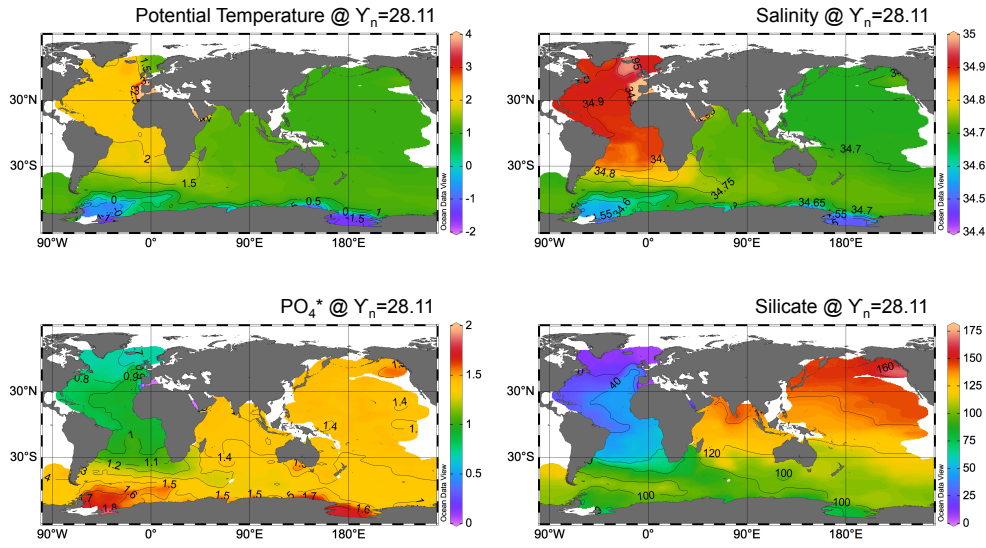


Figure A6: Potential temperature, salinity,  $PO_4^*$ , and silicate on the 28.3 isopycnal horizon. The depth of this horizon is shown in Figure 8 and averages  $\sim 4000$  m in the basins and  $\sim 400$  m in the mixed layer in the Southern Ocean. Data are from GLODAPv2 (Key et al., 2015; Olsen et al., 2016) with profiles, maps, and sections plotted in ODV (Schlitzer 2015).